

FINITE ELEMENT SIMULATION ON EXTERNAL STABILITY OF THE BEARING REINFORCEMENT EARTH WALL

CHERDSAK SUKSIRIPATTANAPONG

*Department of Civil Engineering, Faculty of Engineering and Architecture,
Rajamangala University of Technology Isan, Thailand*

SUKSUN HORPIBULSUK AND AVIRUT CHINKULKIJNIWAT

*School of Civil Engineering, Institute of Engineering,
Suranaree University of Technology, Thailand*

ARUL ARULRAJAH

*Faculty of Science, Engineering and Technology,
Swinburne University of Technology, Australia*

ABSTRACT

The bearing reinforcement is regarded as a cost-effective earth reinforcement. A parametric study on the external stability of the bearing reinforcement earth (BRE) wall was carried out using PLAXIS 2D. The parametric study was performed by varying the foundation conditions (thickness (T) and modulus of elasticity of the weathered crust (E)) and the BRE wall properties (number of transverse members (n), reinforcement length (L), wall height (H) and reinforcement vertical spacing (S_v)). The BRE wall was modeled under a plane strain condition and the reinforcements were modeled using geotextile elements. The settlement is relatively uniform due to the contribution from the high stiffness of bearing reinforcement. The magnitude of settlement of the BRE wall is dependent on E , T , H , irrespective of the BRE properties. The bearing stress distribution is essentially the same even with different E , T , n , S_v . The magnitude of bearing stress is mainly controlled by H . Two lateral movement patterns are found, mainly depending upon the vertical spacing of the bearing reinforcements, S_v , while the magnitude of the lateral movement is strongly dependent upon the modulus of foundation and the BRE wall properties. The inward lateral movement pattern is found for small S_v value while the outward lateral movement pattern is found for large S_v . Smaller maximum lateral movements are found with more number of transverse members, longer bearing reinforcements and smaller S_v .

1. INTRODUCTION

Mechanically stabilized earth (MSE), an engineered composite material has been extensively used for the construction of earth retaining wall and embankment slope in highway engineering works. A MSE wall is inexpensive, It requires a simple construction operation in a shorter period of time, and has been shown to effectively protect the natural environment through its erosion protection and environmental control attributes. Reinforcement in MSE walls can be laid either continuously along the width of the reinforced soil system (grid type) or laid at intervals (strip type). Both grid and strip reinforcements are widely employed around the world, including Thailand, Japan, China and Australia.

Horpibulsuk and Niramitkornburee (2010) have recently introduced a cost-effective earth reinforcement designated as “Bearing reinforcement”. It can be simply installed, conveniently transported, and possesses high pullout and rupture resistances with less steel volume. Fig. 1 shows the typical configuration of a bearing reinforcement, which is composed of a longitudinal member and transverse (bearing) members. The longitudinal member is a steel deformed bar and the transverse members are a set of steel equal angles. The mechanically stabilized earth (MSE) wall by bearing reinforcements is designated as “Bearing Reinforcement Earth (**BRE**) wall” (Horpibulsuk et al., 2011).

In a MSE wall design, an examination of external and internal stability is a routine design procedure. The examination of external stability is generally performed using the conventional method (limit equilibrium analysis) assuming that the composite backfill-reinforcement mass behaves as a rigid body (McGown et al., 1998). The internal stability of a BRE wall deals with the rupture and pullout resistances of the reinforcement. The practical equations for estimating pullout resistance of the bearing reinforcement with different transverse members were proposed by Horpibulsuk and Niramitkornburee (2010); Suksiripattanapong et al. (2013) and Sukmak et al. (2015). Performance of the test BRE wall on a hard ground formation was investigated in the campus of Suranaree University of Technology (SUT) (Horpibulsuk et al., 2010 and 2011). The practical method of designing the BRE wall founded on a hard stratum was subsequently introduced. This method has been adopted to design several BRE walls under the supervision of the Department of Highways, Thailand.

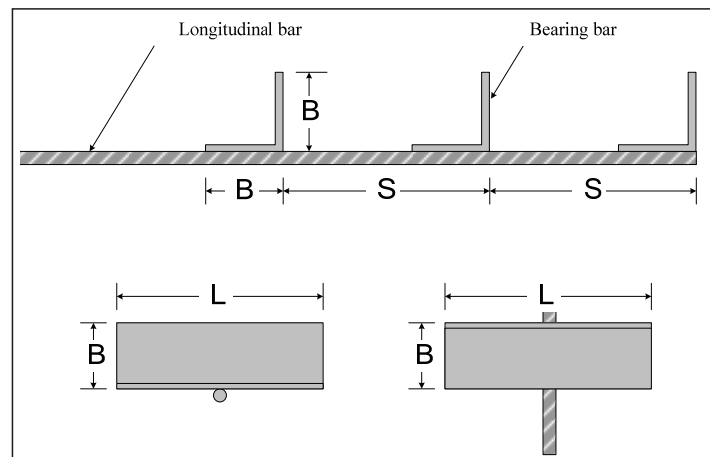


Fig. 1: Configuration of the bearing reinforcement (Horpibulsuk and Niramitkornburee, 2010)

In addition to full-scale tests, the performance of MSE walls was extensively investigated using numerical simulation due to its cost effectiveness (Bergado et al., 2000; Bergado et al., 2003; Bergado and Teerawattanasuk, 2007; Al Hattamleh and Muhunthan, 2006; Hatami and Bathurst, 2006 and Abdelouhab et al., 2011). A numerical study is economical and acceptable if suitable and verified numerical techniques are available. Recently, Suksiripattanapong et al. (2012) used PLAXIS program in the analysis of the performance of BRE wall on a hard ground formation. The simplified method for modeling the bearing reinforcement, which converts the contribution of friction and bearing resistance to the equivalent friction resistance, was subsequently introduced. The performance of the 6 m height BRE wall was successfully simulated. However, their work was limited to the preliminary conceptual stage of the new design method, while the effect of foundation conditions (thickness and modulus of elasticity of the weathered crust) and BRE wall properties (number of transverse members, reinforcement length, wall height and

reinforcement vertical spacing) on the external stability of BRE wall has not been studied and is a novel aspect of this research paper.

This article aims to investigate the effects of foundation conditions and BRE wall properties on the external stability of the BRE wall. The hard foundation is considered in this study on which the BRE wall is typically constructed. The model parameters and the numerical technique proposed by Suksiripattanapong et al. (2012) were adopted for this simulation. The simulation was performed using the finite element code (PLAXIS 2D). The outcome of this study will lead to a fundamental understanding of the effect of various dominant parameters on the external stability of the BRE wall and will also facilitate the engineering decision process in the selection of BRE wall features under a specific in-situ foundation condition of a construction site.

2. FEATURE OF SIMULATED BRE WALL

A simulated BRE wall with 6 m height is illustrated in Fig. 2. The back slope and the wall length at the top of all simulated wall were fixed at 1:1 and 9 m. The wall facing panels were placed on a lean concrete leveling pad (0.15 m width and 0.15 m thickness). The leveling pad was at 0.15 m depth below the excavated ground surface. The wall face was made of segmental concrete panels (1.50 x 1.50 x 0.14 m³).

3. MODEL PARAMETERS

The BRE wall was modeled as a plane strain problem. The finite element mesh and boundary condition are shown in Fig. 2. The finite element mesh involved 15-noded triangular elements for the backfill and the foundation. The simulation was performed under drained condition because of the very deep ground water level. The backfill material was modeled as a linear elastic–perfectly plastic material with the Mohr–Coulomb failure criteria. An elastic, perfectly plastic Mohr–Coulomb model was used to simulate the behavior of the weathered crust layer and medium to very dense sand. The material properties used for the backfill, the weathered crust layer, medium to very dense sand layer for the finite element simulations are shown in Table 1. The parameters are typical of foundation in Northeast Thailand and were obtained from Suksiripattanapong et al (2012).

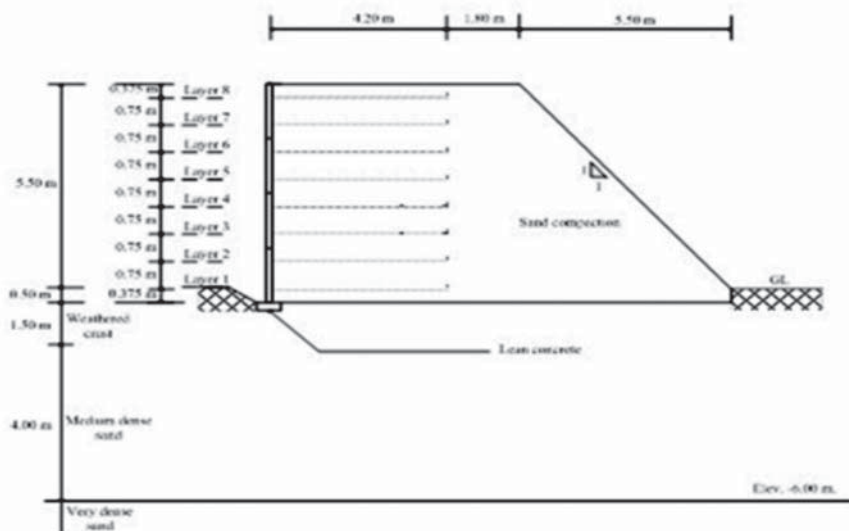


Fig. 2: Schematic diagram of the test wall with instrumentation

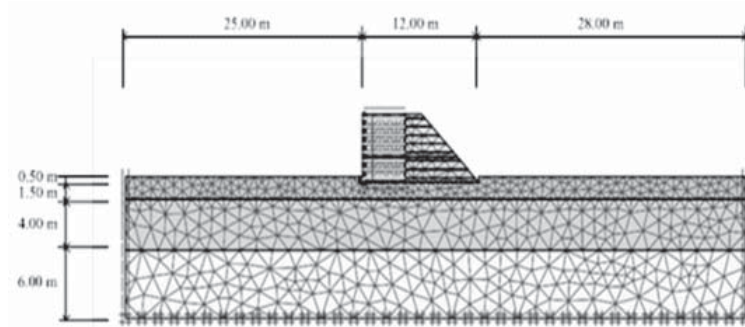


Fig. 3: Finite element model of BRE wall

Table 1: Model parameters for backfill and foundation soils

Item	Backfill soil	Weathered crust	Medium dense sand	very dense sand
Material model	M-C	M-C	M-C	M-C
Material type	Drained	Drained	Drained	Drained
γ_{dry} (kN/m ³)	17	17	17.15	18
E_{ref} (kPa)	35000	1575-2175	40000	50000
ν'	0.33	0.30	0.25	0.25
c' (kPa)	1	20	1	1
ϕ (°)	40	26	35	38
Ψ (°)	8	0	3	8

Geotextile elements, which cannot resist bending moment, were adopted to model the bearing reinforcement, even though it is composed of longitudinal and transverse members as proposed by Suksiripattanapong et al. (2012). The facing panel was modeled as a beam element. The parameters for bearing reinforcement and facing panel used in the BRE wall model are shown in Table 2.

Table 2: Model parameters for reinforced element structure

Item	Bearing reinforcement	Facing concrete
Material model	Elastic	Elastic
EA, (kN/m)	4.5E+4	3.556E+6
EI, (kNm ² /m)	-	5808
W, (kN/m/m)	-	3.36
ν'	-	0.15

4. METHODOLOGY

The BRE wall is generally constructed on the weathered crust layer, which is more compressible than the underlying subsoil. Therefore, the thickness and modulus of the weathered crust layer will affect the BRE wall performance. The parametric studies on lateral movement of BRE walls were performed

by varying the thickness, T and modulus, E of the weathered crust while other parameters of BRE wall properties were kept constant. The thicknesses of the weathered crust were 1.5, 2.0 and 2.5 m, which are commonly found in the field. The E values were 1,575, 1,875 and 2,175 kPa, which are representative of soft to stiff weathered crust. The BRE wall properties include the number of transverse members, n , reinforcement length, L , wall height, H and vertical spacing, S_v . The interaction coefficient between bearing reinforcement and backfill soil, R was used to simulate the number of transverse members, which can simply be obtained from the curve fitting of laboratory pullout test results. The details of obtaining the R value can be referred to Suksiripattanapong et al. (2012). It was shown that the R value increases with the number of transverse members. The R values of 0.55, 0.65, 0.75 and 0.85 were suggested for 1, 2, 3 and 4 transverse members, respectively (Suksipattanapong, 2013 and Suksiripattanapong et al., 2012). These values were suggested for transverse member with 25 mm (B) and 180 mm (W) (refer to Fig. 1). The effect of reinforcement length on the performance of BRE wall was illustrated by comparisons of simulation results of cases 31 to 34. The reinforcement lengths were varied between 4.2 and 6 m. The effect of wall height on the performance of BRE wall was depicted by comparisons of simulation results of cases 31, 35 and 39. The wall heights were 6.0, 7.5 and 9.0 m. The minimum reinforcement length for the simulation was 70% of the wall height as recommended for designing of MSE walls by AASTHO (2002). Therefore, the studied reinforcement lengths were 4.2, 5.25 and 6.3 m. The variations of vertical spacing were 0.5, 0.75 and 1.0 m (cases 31 and 43 to 62). In total, 62 cases were run in this detailed parametric study.

5. SIMULATED RESULTS

5.1 Settlement

The numerical settlements of the BRE wall under different foundation and wall properties are illustrated in Fig 4. The thickness of weathered crust, T , modulus of elasticity of weathered crust, E and wall height, H significantly affect the magnitude of settlement as illustrated by comparisons of the simulation results of cases 1 to 5, and 31, 35 and 39. It is of interest to note that the maximum settlement is found at the front of the wall base and beyond this region, the settlement is relatively uniform for different E and T values. The uniform settlement is contributed from the high stiffness of the bearing reinforcements. The number of transverse members, n , reinforcement length, L , and vertical spacing, S_v , insignificantly affect the settlement as seen by the simulated results of cases 28 to 34, and 31, 43 and 44.

5.2 Bearing Stress

The simulated distributions of bearing stresses at the end of construction, from the front to the back and for different weathered crust and BRE wall properties are shown in Fig 5. For all the simulation cases, the stress distribution is uniform for the distance of larger than 1.0 m from the facing. The relatively high bearing stress at the front of the wall is caused by the concentrated load from the wall facing. For the same H , the stress distribution pattern and magnitude are essentially the same for different E and T (cases 4, 2, and 5 and cases 1 to 3), n (cases 28 to 30) and S_v (cases 31, 43 and 44) values. A more uniform stress distribution is found for longer reinforcements due to lower eccentric loads on the foundation.

The effect of wall height on the bearing stress distribution is clearly observed by a comparison of the cases 31, 35 and 39 for the heights of 6.0, 7.5 and 9.0 m. In the analysis, the reinforcement length was increased with the increase in wall height for the external stability. The maximum bearing stress at the wall front increases significantly as the wall height increases. It is evident that in the linear elastic analysis, the bearing stress distribution is strongly dependent upon H and L , regardless of T , E , R and S_v .

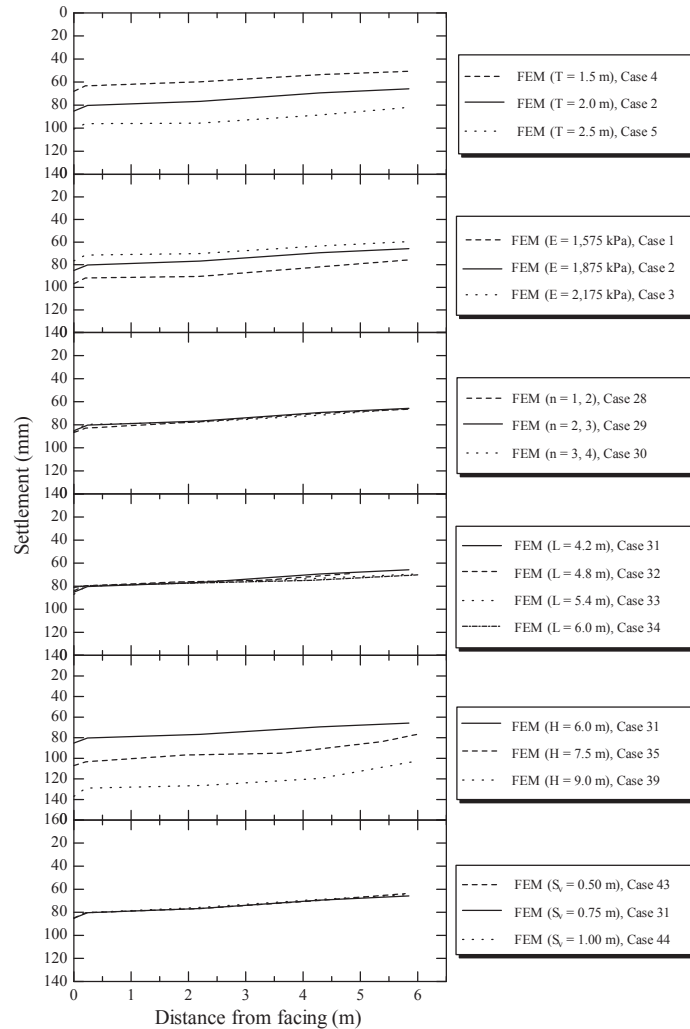


Fig. 4: Effects of T , E , n , L , S_v and H on settlement pattern.

5.3 Lateral Movements

The simulated lateral movements are compared and shown in Figs 6-9 for different properties of weathered crust and BRE wall. The effect of the vertical spacing of the reinforcement, S_v on the lateral movement pattern is shown in these figures for S_v values of 0.5, 0.75 and 1.0 m. Two patterns are found: inward and outward lateral movement. For the smallest S_v value of 0.5 m, the inward lateral movement pattern is found with the maximum movement at about 1/3 of the wall height. The maximum movement is found approximately between the mid and the top of the wall height for larger S_v values and the location of the maximum movement moves toward the top of the wall with the increase in S_v value.

The effect of T and E on the lateral movement for both patterns is illustrated by a comparison of simulated results of cases 2, 4, 5 and 43 to 48 and of cases 1 to 3, 43, 44, and 49 to 52 (refer to Figs 6 and 7). The lateral movement at the wall base increases as T increases and E decreases, resulting in the increase

in overall lateral movements. For a particular T and E , the S_v value controls the magnitude of lateral movement. The lower S_v value increases stiffness of the composite mass and then leads to lower overall lateral movement. The effect of the number of transverse members (interaction coefficient, R) on the lateral movement is shown in Figure 8 for both patterns. The study is in nine cases for the S_v values of 0.5, 0.75 and 1.0 m and the R values of 0.55, 0.65, 0.75 and 0.85. Case 28, 53 and 55 are for R values of 0.55 ($n = 1$) and 0.65 ($n = 2$) for 1st to 3rd and 4th to 8th reinforcement layers, respectively. Case 2, 43 and 44 are for R values of 0.65 ($n = 2$) and 0.75 ($n = 3$) for 1st to 3rd and 4th to 8th reinforcement layers, respectively. Case 30, 54 and 56 are for R values of 0.75 ($n = 3$) and 0.85 ($n = 4$) for 1st to 3rd and 4th to 8th reinforcement layers, respectively. For all the cases, the change in the lateral movement at the wall base is insignificant even with the difference in R and S_v values since it is controlled by E and T . For each S_v case, the lateral movements decrease with an increase in n due to the increase in the pullout resistance (Suksiapattanapong et al., 2013). As such, the increase in n not only increases the factors of safety against pullout failure but also reduces the lateral movement significantly.

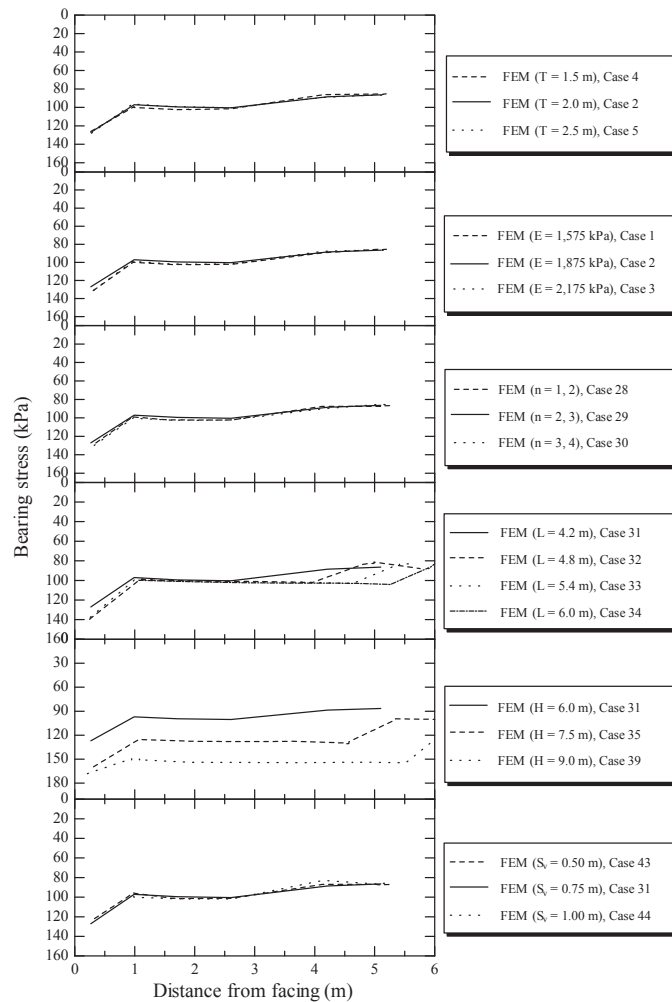


Fig. 5: Effects of T , E , n , L , S_v , and H on bearing stress distribution.

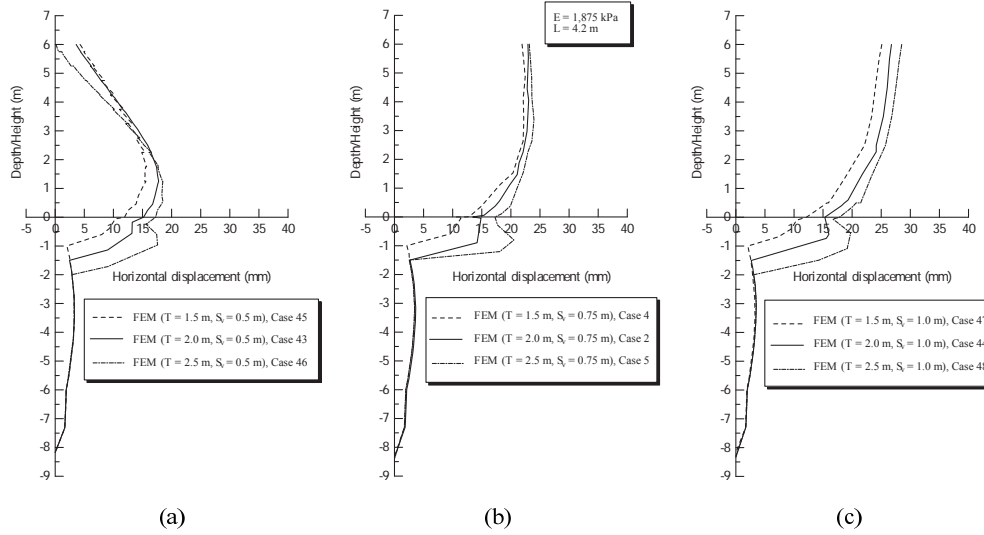


Fig. 6: Effect of weathered crust thickness, T on lateral movement.

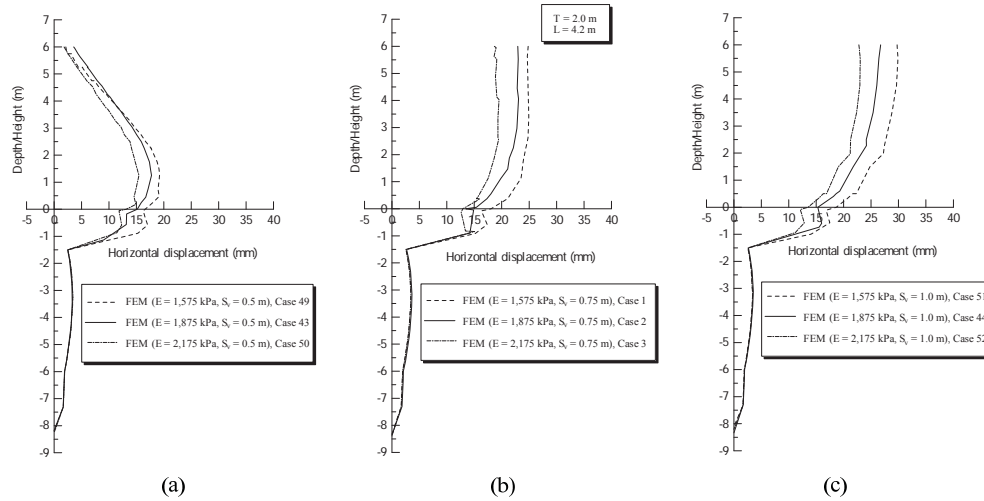


Fig. 7: Effect of modulus of elasticity of the weathered crust, E on lateral movement.

Fig 9 shows the effect of the reinforcement length, on the lateral movement by a comparison of simulated results of cases 31 to 34, 43, 44 and 57 to 62. The minimum reinforcement length for MSE wall is recommended to be 70% of the total height of the wall (AASTHO, 2002). The L/H ratios were 0.7, 0.8, 0.9 and 1.0 for this parametric study. The L/H ratio of 1.0 gives maximum lateral displacement lower than the L/H ratio of 0.7 by about 23%, 10% and 15 % for the S_v values of 0.5, 0.75 and 1.0 m, respectively. The reduction in lateral movement is because the increase in the pullout resistance (increase in the embedded length in the passive zone). The lateral movements are essentially the same when value is greater than 0.8. Consequently, the increase in n is more advantage in term of lateral movement and cost effectiveness than the increase in L for a particular H and S_v .

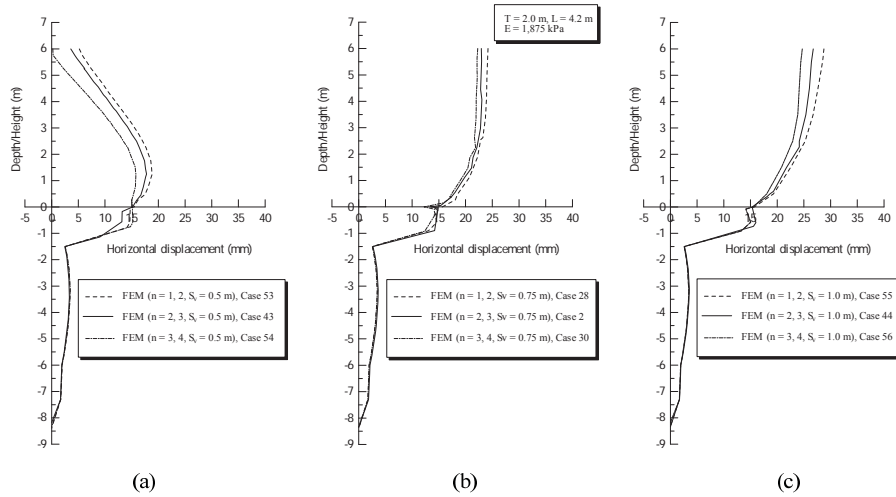


Fig. 8: Effect of number of transverse members, n on lateral movement.

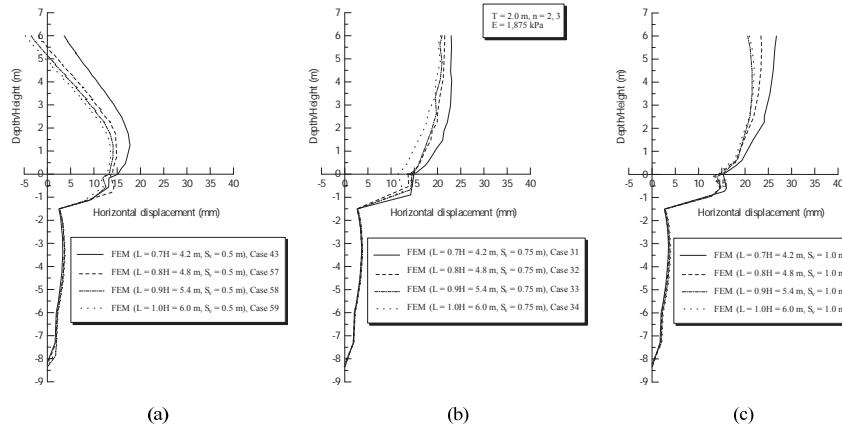


Fig. 9: Effect of reinforcement length, L on lateral movement

6. CONCLUSIONS

The parametric numerical studies on BRE wall were performed by varying the foundation conditions (T and E) and the BRE wall properties (n , L , H and S_v). The following conclusions can be drawn from this parametric study:

1. Due to the large stiffness of reinforcement, the settlement of the BRE wall is relatively uniform. The magnitude of settlement is dependent on E , T and H , irrespective of the BRE wall properties.
2. For L/H ratios greater than 0.7 as recommended by AASHTO (2002), n , E and T do not control the pattern and magnitude of bearing stress distribution. The stress distribution is more uniform with longer reinforcement length owing to lower eccentric load on the foundation. The magnitude of bearing stress is strongly dependent upon H .
3. The vertical spacing controls the lateral movement pattern. The inward movement is found for $S_v < 0.5$ m and the outward movement is found for $S_v > 0.5$ m. The maximum lateral movement is larger

for larger S_v value. The maximum movement occurs between mid and top of the wall height for the S_v values greater than 0.5 and moves toward the top of the wall with increasing the S_v value.

4. For a particular S_v value and wall height, the maximum lateral movement is controlled by foundation properties (E and T), n and L . The lower the E and the thicker the T , the larger the lateral movement at the wall base. This results in larger maximum lateral movement. The more the n and the longer the L , the higher the pullout resistance. This higher pullout resistance increases not only the factor of safety but also the lateral movement. Instead of increasing L , the increase in n is more advantage in term of lateral movement and factor of safety because the lateral movement is essentially the same when L/H ratio is greater than 0.8.

REFERENCES

- AASHTO (2002). Standard specifications for highway and bridge, seventh ed. American Association of State Highway and Transportation Officials, Washington D.C.
- Abdelouhab, A., Dias, D. and Freitag, N. (2011). Numerical analysis of the behaviour of mechanically stabilized earth walls reinforced with different types of strips. *Geotextiles and Geomembranes* (29): 116-129.
- Al Hattamleh, O. and Muhunthan, B. (2006). Numerical procedures for deformation calculations in the reinforced soil walls. *Geotextiles and Geomembranes* 24(1): 52-57.
- Bergado, D.T. and Teerawattanasuk, C. (2007). 2D and 3D numerical simulations of reinforced embankments on soft ground. *Geotextiles and Geomembranes* 26(1): 39-55.
- Bergado, D.T., Teerawattanasuk, C., Youwai, S. and Voottipruex, P. (2000). FE modeling of hexagonal wire reinforced embankment on soft clay. *Canadian Geotechnical Journal* 37(6): 1-18.
- Bergado, D.T., Youwai, S., Teerawattanasuk, C. and Visudmedanukul, P. (2003). The interaction mechanism and behavior of hexagonal wire mesh reinforced embankment with silty sand backfill on soft clay. *Computers and Geotechnics* 30: 517-534.
- Hatami, K. and Bathurst, R.J. (2006). Numerical model for the analysis of geosynthetic-reinforced soil segmental wall under surcharge loading. *Journal of Geotechnical and Geoenvironmental Engineering* 136(6): 673-684.
- Horpibulsuk, S. and Niramitkornburee, A. (2010). Pullout resistance of bearing reinforcement embedded in sand. *Soils and Foundations* 50(2): 215-226.
- Horpibulsuk, S., Suksiripattanapong, C. and Niramitkornburee, A. (2010). A method of examining internal stability of the bearing reinforcement earth (BRE) wall. *Suranaree Journal of Science and Technology* 17(1): 1-11.
- Horpibulsuk, S., Suksiripattanapong, C., Niramitkornburee, A., Chinkulkijniwat, A. and Tangsutinon, T. (2011). Performance of earth wall stabilized with bearing reinforcements. *Geotextiles and Geomembranes* 29(5): 514-524.
- McGown, A., Andrawes, K.Z., Pradhan, S. and Khan, A.J. (1998). Limit state analysis of geosynthetics reinforced soil structures. Keynote lecture. In: *Proceedings of 6th International Conference on Geosynthetics*, March, 25-29, 1998, Atlanta, GA, USA. 143-179.
- Rowe, R.K. and Ho, S.K. (1997). Continuous panel reinforced soil walls on rigid foundations. *Journal of Geotechnical and Geoenvironmental Engineering* 123(10): 912-920.
- Skinner, G.D. and Rowe, R.K. (2005). Design and behavior of a geosynthetic reinforced retaining wall and bridge abutment on a yielding foundation. *Geotextiles and Geomembranes* 23(3): 234-260.

- Suksiripattanapong, C. (2013). Pullout Resistance of Bearing Reinforcement and Finite Element Analysis of Bearing Reinforcement Earth Wall. Ph.D. Thesis. Suranaree University of Technology, Thailand.
- Sukmak, K., Sukmak, P., Horpibulsuk, S., Han, J., Shen, S.L., and Arulrajah, A. (2015). Effect of fine content on the pullout resistance mechanism of bearing reinforcement embedded in cohesive-frictional soils. *Geotextiles and Geomembranes*. 43: 107-117.
- Suksiripattanapong, C., Chinkulkijniwat, A., Horpibulsuk, S., Rujikiatkamjorn, C. and Tangsuttinon, T. (2012). Numerical analysis of bearing reinforcement earth (BRE) wall. *Geotextiles and Geomembranes* 32: 28-37.
- Suksiripattanapong, C., Horpibulsuk, S., Chinkulkijniwat, A. and Chai, J.C. (2013). Pullout resistance of bearing reinforcement embedded in coarse-grained soils. *Geotextiles and Geomembranes* (36): 44-54.